Interrelations Between Elastic Energy and Strain in a Tensegrity Model: Contribution to the Analysis of the Mechanical Response in Living Cells

Sylvie Wendling-Mansuy, Patrick Canadas, Christian Oddou, Alain Meunier

Interrelations Between Elastic Energy and Strain in a Tensegrity Model: Contribution to the Analysis of the Mechanical Response in Living Cells

SYLVIE WENDLING[a,*], PATRICK CAÑADAS[a,b], CHRISTIAN ODDOU[a] and ALAIN MEUNIER[c]

[a]Laboratoire de Mécanique Physique, Université Paris 12, Créteil, France
[b]INSERM U-492, Université Paris 12, Créteil, France
[c]Laboratoire de Recherches Orthope´diques, Université Paris 7, Paris (CNRS ESA 7052), France

Interactions between the physical and physiological properties of cellular sub-units result in changes in the shape and mechanical behaviour of living tissues. To understand the mechanotransmission processes, models are needed to describe the complex interrelations between the elements and the cytoskeletal structure. In this study, we used a 30-element tensegrity structure to analyse the influence of the type of loading on the mechanical response and shape changes of the cell. Our numerical results, expressed in terms of strain energy as a function of the overall deformation of the tensegrity structure, suggest that changes in cell functions during mechanical stimuli for a given potential energy are correlated to the type of loading applied, which determines the resultant changes in cell shape. The analysis of these cellular deformations may explain the large variability in the response of bone cells submitted to different types of mechanical loading.

Keywords: Pre-stress; Structural model; Strain energy; Mechanotransmission; Cytoskeleton

INTRODUCTION

Living tissues contain many different types, shapes and sizes of cells, all of which have similar physical properties, suggesting that there are underlying universal rules for cellular and tissue organisation. Most of these cell types can respond to physiological mechanical stresses and can alter their architectural and functional features in response to externally applied loads [1–3]. For example, the shape, apparent density and stiffness of bone continually change in response to their environmental load [4]. However, the cellular mechanisms constituting the mechanosensory system in bone tissue and driving adaptive remodelling have not yet been fully elucidated. Similarly, cells continually respond to their environmental load. The various modes of loading of the extracellular matrix (stress or strain fields, fluid pressure, interstitial fluid flow) induce a series of biophysical coupled events in cells that affect the overall response of the chondrocytes (changes in cell shape and volume, deformation of the membrane, cytoskeleton, organelles and nucleus) [5,6].

However, the cell mechanotransduction phenomena are complex and not well understood. In fact, changes in cell shape depend on several factors. Many authors have shown that (i) cellular stress–strain relationships are non-linear (the stiffness of the cells increases with applied stress) [7,8] and that (ii) the cell shape is defined by the geometrical and mechanical properties of the cytoskeleton filaments and by the microenvironment (extracellular matrix–cell and/or cell–cell attachment conditions, mechanical stress applied) [9,10]. To determine the inherent factors that characterise the non-linear mechanical behaviour of living cells, we developed a model based on tensegrity structures. These self stress spatial structures have been proposed to describe the relationship between the shape, functions and structure of living cells [11]. We analysed the variations of strain energy in a 30-element tensegrity structure that was submitted to major deformations and to different types of loading. To determine the relationships that reflect the non-linear mechanical behaviour of such a tensegrity structure in terms of strain energy and energy level variations, it is necessary to understand and

*Corresponding author.

to generalise the mechanical response of living cells submitted to different types of loading.

THEORETICAL TENSEGRITY MODEL

Definition of the 30-element Tensegrity Structure in the Reference State

The spatial tensegrity structure studied is composed of six rigid elements (bars) compressed by 24 pre-stretched elastic elements (cables) (Fig. 1). Both constitutive elements (p) are defined by their geometry (length l_p, radius r_p, cross-sectional area S_p ($=\pi r_p^2$)), and by their mechanical properties (Young's modulus E_p). T_c is the stretching force in the cables and T_b is the compressing force in rigid bars. The radius and Young's modulus of both elements and the length of the bars are considered to be constant during the overall deformation of the tensegrity structure.

In the reference state (i.e. in the absence of external forces) the geometrical symmetry of the structure, in which the bars are aligned in pairs in three perpendicular spatial planes, implies the following relationship between the length of the bars, l_b, and the length of the cables, l_c, (exponent (r) means reference state) [12]:

$$\frac{l_c^{(r)}}{l_b} = \sqrt{3/8}. \tag{1}$$

The internal tension of the structure is characterised by the tension in the elastic cables, the mechanical behaviour of which is believed to be linear. This tension depends on the state of deformation (ε_c) and the physical properties (Young's modulus E_c and cross-sectional area S_c) of a given cable:

$$T_c = E_c S_c \varepsilon_c. \tag{2}$$

In the reference state the tension, T_c, is similar in every cable in the structure. The stability of the tensegrity structure shape is obtained from the internal forces equilibrium and a constant ratio between the compression of the rigid bars and the tension of the elastic cables [13].

Nodal Attachment Conditions and Forces Applied to the 30-element Tensegrity Structure

We submitted the 30-element tensegrity model to four different types of loading (extension–compression, shear and torsion) and analysed the resulting large deformations. The structure was always anchored to a rigid base by spherical joints at the three inferior nodes {#1, #2, #3}. The rectangular base $\{\vec{i},\vec{j},\vec{k}\}$ constituted the referential system. When the structure was extended or compressed, the three superior nodes {#10, #11, #12} move along the k-axis. When the structure was exposed to shear stress these three nodes moved along the j-axis and formed a superior plane that remained parallel to the $\{\vec{i},\vec{j}\}$ plane.

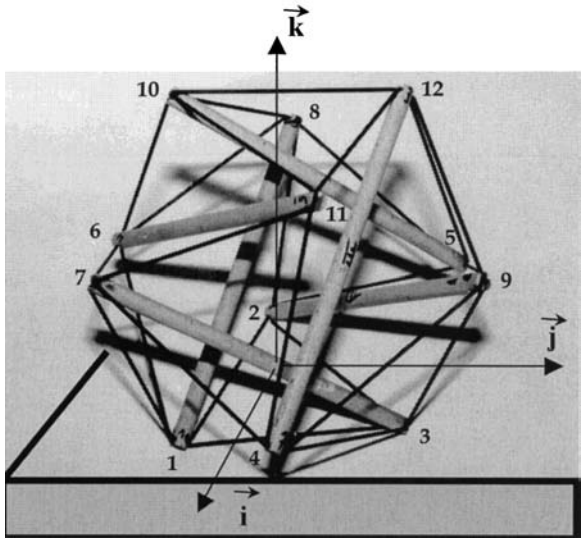

FIGURE 1 Tensegrity structure composed of six rigid bars compressed by 24 pre-stretched elastic cables. The structure is attached to a rigid substratum by three nodes {#1, #2, #3}, which define the inferior plane. The nodes {#10, #11, #12} define the superior plane, which is parallel to the inferior plane.

During torsion this superior plane rotated around the k-axis and remained parallel to the $\{\vec{i},\vec{j}\}$ plane.

The strain energy of the overall structure was deduced from the resolution of the following equations:

$$\{\mathbf{F}\} = [\mathbf{K}]\{\mathbf{u}\}. \tag{3}$$

This describes the equilibrium between the internal and external forces applied to the nodes and takes into account the mechanical and geometrical properties of the constitutive elements (bars and cables) and the compatibility between small nodal displacements and the deformation of the elements [14]. The components of the column vector $\{\mathbf{F}\}$ (dimension $[1 \times 36]$) are the external forces (null or unknown) applied on the 12 nodes of the structure in the three spatial directions. The components of the column vector $\{\mathbf{u}\}$ (dimension $[1 \times 36]$) are the imposed small nodal displacements in the three directions. The overall rigidity matrix $[\mathbf{K}]$ (dimension $[36 \times 36]$) is assembled from each elementary rigidity matrix $[\mathbf{K}]_p$ which depends exclusively on the Young's Modulus E_p, the internal force T_p (i.e. tension in the cables, compression in the bars), cross-sectional area S_p and the length l_p of the element (p) as following:

$$[\mathbf{K}]_p = \begin{bmatrix} \frac{E_p \cdot S_p - T_p}{l_p} c_x^2 + \frac{T_p}{l_p} & & \text{symmetrical} \\ \frac{E_p \cdot S_p - T_p}{l_p} c_x \cdot c_y & \frac{E_p \cdot S_p - T_p}{l_p} c_y^2 + \frac{T_p}{l_p}; & \\ \frac{E_p \cdot S_p - T_p}{l_p} c_x \cdot c_z & \frac{E_p \cdot S_p - T_p}{l_p} c_y \cdot c_z & \frac{E_p \cdot S_p - T_p}{l_p} c_z^2 + \frac{T_p}{l_p} \end{bmatrix}. \tag{4}$$

where the position of the element (p) as a result of the spatial organisation of the structure are taken into account by the elementary director cosines (c_x, c_y and c_z).

Equation (3) defines small deformations in the structure. The large deformation resolution used a linear incremental method, which consisted of incrementing the large displacement imposed and re-initialising the parameters of Eq. (3) at each increment (see [14] and Appendix in Ref. [15]). The strain energy of the overall structure is calculated at each increment and is expressed as follows:

$$\mathbf{W} = \{\mathbf{F}\}\cdot\{\mathbf{u}\}. \tag{5}$$

The apparent strain of the overall tensegrity structure was calculated from the relative displacement ($\Delta\mathbf{u}$) of the superior plane along the imposed k-axis direction in extension–compression (and the j-axis during shear):

$$\varepsilon = \frac{\Delta\mathbf{u}}{L^{(\mathrm{r})}}. \tag{6}$$

divided by the distance in the reference state ($L^{(\mathrm{r})}$)(before deformation) between the inferior and superior plane. During shear, extension and compression the relative displacement of the superior plane is related to the displacement of the nodes {#10, #11, #12}. During torsion the overall strain, ε, is defined by the angular displacement of these three nodes in a plane parallel to the $\{\vec{i},\vec{j}\}$ plane. These angular variations are the same for the three nodes. In this study, the displacements of the other free nodes are not considered and the displacements of the nodes {#10, #11, #12} in non-imposed directions are equal to zero.

RESULTS

The numerical results are expressed in terms of the normalised strain energy, W^*, as a function of the overall deformation of the tensegrity structure. By definition, the strain energy of the overall structure is normalised by the elastic energy of a given cable strained at 100% of its free length. Figure 2 shows the variation of the normalised strain energy of the 30-element tensegrity structure submitted to four different types of loading (extension–compression, shear and torsion). The internal tension of this structure is given by the normalised elastic tension, T^* (=0.005), which corresponds to the extension, ε_c, of the cables (see Eq. 2) in the reference state of the tensegrity structure (before loading). The size of the structure tested was considered to be constant ($l_b = 200$ mm). During the four different types of loading, the normalised strain energy of the structure varied non-linearly with its overall deformation. This non-linearity differed for each of the four loading conditions; the slope of strain energy–deformation is greater during extension than during shear or torsion and this slope is inversed during compression, i.e. the tensegrity structure became smoother during compression and harder during extension.

For the four modes of loading, the strain energy levels appeared to vary when the structure underwent large deformations ($\varepsilon > 30\%$). These different levels of energy correspond to the differences between the type of loading but identical states of deformation of the tensegrity structure. During small deformations ($\varepsilon < 5\%$), the strain energy of the structure seemed to remain unchanged regardless of the type of loading. It is noteworthy that during the overall deformation of the 30-element tensegrity structure, the elastic cables were spatially organised so that some of them were stretched and some of them were slack. Figure 3 shows the "Normalised strain energy–strain" relationships, expressed on a logarithmic scale for three different values of internal tension T^*

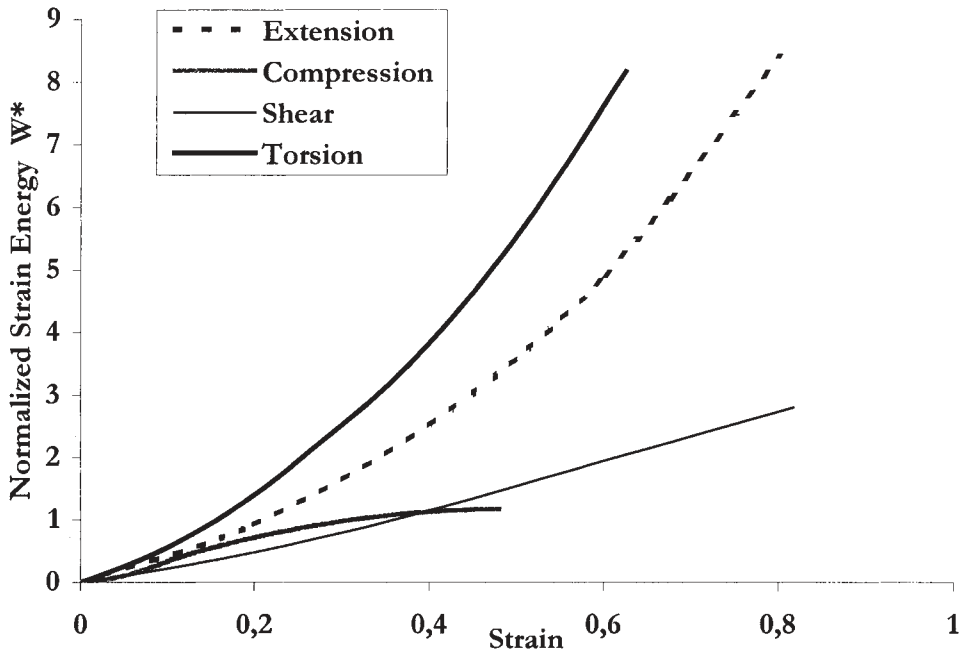

FIGURE 2 Numerical results: Normalised strain energy, $\mathbf{W}^*$, as a function of the overall strain of a 30-element tensegrity structure (length of the bars; $l_b = 200$ mm and normalised internal tension; $T^* = 0.005$) submitted to extension–compression, shear and torsion.

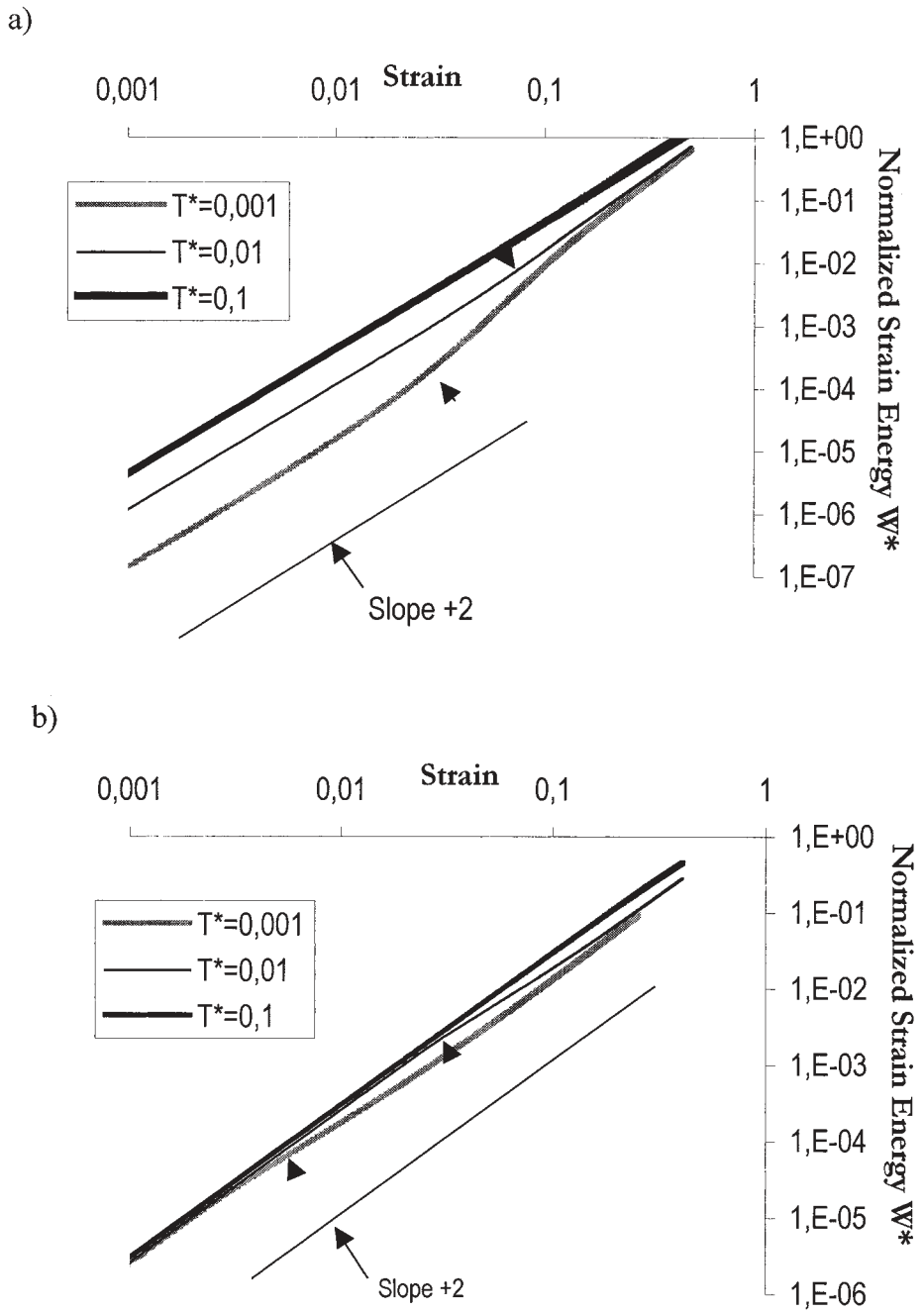

FIGURE 3 Numerical results in log–log scale: Normalised strain energy as a function of the overall strain of the 30-element tensegrity structure submitted to (a) extension and (b) shear, for three values of internal tension ($T^* = 0.001$, 0.01 and 0.1).

(=0.001, 0.01, 0.1) of the 30-element tensegrity structure. It appears that the normalised strain energy of the tensegrity structure increases with the initial tension regardless of the type of loading. Moreover, following small deformations, the strain energy is a quadratic function of the overall strain of the structure (slope +2, Fig. 3a,b) regardless of the level of internal tension in extension (Fig. 3a) and in shear (Fig. 3b). This quadratic relationship is similar to those obtained for an equivalent continuum medium during small deformations. Therefore, it appears that the non-linearity of the ($\mathbf{W}^* - \varepsilon$) relationship differs for each type of loading and level of internal tension of the tensegrity structure. This non-linearity threshold seems to appear at overall strain values that decrease with internal tension (see arrows in Fig. 3). It is noteworthy that non-linearity does not appear for large values of internal tension ($T^* = 0.1$) during shearing or extension.

DISCUSSION

Based on Ingber's [11] proposal that changes in cellular shape are closely related to the structural reorganisation of

the cytoskeleton (CSK), we developed a theoretical model based on tensegrity structures that can describe the global mechanical properties of the cytoskeletal structure as a function of the geometrical and mechanical properties of the constitutive filaments (microtubules, microfilaments and intermediate filaments). Indeed, the overall deformation of the tensegrity structure depends on the rearrangement of the constitutive rigid bars (microtubules associated with intermediate filaments) compressed by pre-stretched cables (microfilaments and/or stress fibres) and this rearrangement results from the equilibrium between internal tension and the external forces applied by the environmental medium. We previously showed that the 30-element tensegrity structure, comprising six rigid bars and 24 elastic cables, presents a non-linear "stress–strain" relationship that depends strongly on internal tension, structural size (or length of the rigid elements) and the type of loading [15,16].

In this study, we tried to identify the inherent factors that determine the non-linearity of the mechanical response of a 30-element tensegrity structure submitted to four different types of loading (extension–compression, shear and torsion). The numerical results obtained from the resolution of a system of equations that traduce the equilibrium forces at each node of the tensegrity structure are expressed in terms of global strain energy. This structural strain energy permits the normalisation of the macroscopic mechanical behaviour of the tensegrity model, which is non-linear and highly heterogeneous.

The numerical results show that the non-linear behaviour of the 30-element tensegrity model appears essentially following large deformations ($\varepsilon > 10\%$) but that the threshold of this non-linearity depends on the type of loading and the level of internal tension of the structure. During each type of loading the elastic cables of the structure are stretched differently, some of them are extended and others are slack. The number of stretched cables, and the direction and amplitude of extension vary in the four types of loading. The rigid bars also moved in different directions and amplitudes with the different types of loading. Thus, the variations in the non-linearity of the mechanical behaviour of tensegrity structures are characteristic of the structural heterogeneity and result from (i) the so called "geometrical" non-linearity due to the spatial reorganisation and mobility of the constitutive rigid elements which predominate the linear deformation of the elastic cables and (ii) the so called "material" non-linearity due to the extension of some elastic cables and not others during the overall deformation of the structure. Thus, this geometrical non-linearity is more important and selective considering the type of loading when the pre-stress is weak.

The mechanical behaviour of cultured cells is known to be highly non-linear and multifactorial [7,17]. Cellular stiffness increases with the applied stress [18], this stiffness closely depends on the cell–cell and/or cell–extracellular matrix attachment conditions and the type of stress applied. Interestingly, rigid tensegrity structures (great internal tension) do not present a non-linear mechanical behaviour. In contrast, tensegrity structures with a weak internal tension (T^* in the order of 10^{-3}) present a non-linearity that appears following a small overall deformation (5%). Internal tension values corresponding to normalised elastic tension (T^*), in the order of 10^{-3} similar to those of the tensegrity model have also been observed in cultured cells whose mechanical response is non-linear [19].

The results obtained by our 30-element tensegrity model suggest that the changes in cellular functions that occur during mechanical stimuli are correlated, for a given level of strain energy, to the type of loading that determines the cell shape modifications. These results should allow us to interpret the changes in the internal energy of the cell induced by cellular adhesion during the differentiation processes that bone cells undergo. This tensegrity model might be useful for the quantification of the average strain energy of living cells and for comparison with the average energy spent during cellular metabolism.

This generalised tensegrity model, which also applies to more complex tensegrity structures that implicate energetic and chemical environmental exchanges, might enable us to evaluate the coupling between cellular energy, shape and functions in every biochemical, mechanical or thermodynamical process.

References

[1] Sachs, F. (1988) "Mechanical transduction in biological systems", *Critical Review in Biomedical Engineering* **16**(2), 141–169.

[2] Hackney, C.M. and Furness, D.N. (1995) "Mechanotransduction in vertebrate hair cells: structure and function of the stereociliary bundle", *American Journal of Physiology* **268**, c1–c13.

[3] Harris, R., Kondo, S. and Yasuda, T. (1997) "Mechanical stress-cell function relationships in renal cells", *Experimental Nephrology* **5**, 263–270.

[4] Turner, C.H. and Pavalko, F.M. (1998) "Mechanotransduction and functional response of the skeleton to physical stress: the mechanisms and mechanics of bone adaptation", *Journal of Orthopaedic Science* **3**, 346–355.

[5] Guilak, F. (1995) "Compression-induced changes in the shape and volume of the chondrocyte nucleus", *Journal of Biomechanics* **28**(12), 1529–1541.

[6] Takano, Y., *et al.*, (1999) "Elastic anisotropy and collagen orientation of osteonal bone are dependent on the mechanical strain distribution", *Journal of Orthopaedic Research* **17**, 59–66.

[7] Wang, N., Butler, J. and Ingber, D. (1993) "Mechanotransduction across the cell surface and through the cytoskeleton", *Science* **260**, 1124–1127.

[8] Fung, Y.C., Liu, S.Q. and Zhou, J.B. (1993) "Remodelling of the constitutive equation while a blood vessel remodels itself under stress", *Journal of biomechanical engineering* **115**(4B), 453–459.

[9] Bereiter-Hahn, J., Anderson, O.R. and Reif, W.E. (1987) Cytomechanics: the Mechanical Basis of Cell Form and Structure, 294th ed. (Springer).

[10] Ingber, D.E. (1997) "Tensegrity: the architectural basis of cellular mechanotransduction", *Annual Review of Physiology* **59**, 575–599.

[11] Ingber, D. (1993) "Cellular tensegrity: defining new rules of biological design that govern the cytoskeleton", *Journal of Cell Science* **104**, 613–627.

[12] Kenner, H. (1976) In: Geodesic Math and How to Use It (University of California Press).

[13] Mohri, F. and Motro, R. (1993) "Static and kinematic determination of generalized space reticulated systems", *Structural Engineering Review* **5**(3), 231–237.

[14] Argyris, J.H. and Scharpf, D.W. (1972) "Large deflection analysis of prestressed networks", *Journal of the Structural Division* **106**(3), 633–654.

[15] Wendling, S., Oddou, C. and Isabey, D. (1999) "Stiffening response of a cellular tensegrity model", *Journal of Theoretical Biology* **196**(3), 309–325.

[16] Wendling, S., *et al.*, (2000) "Role of cellular tone and microenvironmental conditions on cytoskeleton stiffness assessed by tensegrity model", *European Physics Journal AP* **9**, 51–62.

[17] Thoumine, O., *et al.*, (1995) "Elongation of confluent endothelial cells in culture: the importance of fields of force in the associated alterations of their cytoskeletal structure", *Experimental Cell Research* **219**, 427–441.

[18] Laurent, V., *et al.*, (1998) "Mesure de la rigidité cellulaire par magnétocytométrie", *Archives of Physiology and Biochemistry* **106**, 183.

[19] Gittes, F., *et al.*, (1993) "Flexural rigidity of microtubules and actin filaments measured from thermal fluctuations in shape", *The Journal of Cell Biology* **120**, 923–934.